

# The Type IX Secretion System and Its Role in Bacterial Function and Pathogenesis

Journal of Dental Research  
1–10  
© International Association for Dental Research and American Association for Dental, Oral, and Craniofacial Research 2021  
Article reuse guidelines:  
sagepub.com/journals-permissions  
DOI: 10.1177/00220345211051599  
journals.sagepub.com/home/jdr

P.D. Veith<sup>1</sup>, M.D. Glew<sup>1</sup>, D.G. Gorasia<sup>1</sup>, E. Cascales<sup>2</sup>, and E.C. Reynolds<sup>1</sup>

## Abstract

*Porphyromonas*, *Tannerella*, and *Prevotella* species found in severe periodontitis use the Type IX Secretion System (T9SS) to load their outer membrane surface with an array of virulence factors. These virulence factors are then released on outer membrane vesicles (OMVs), which penetrate the host to dysregulate the immune response to establish a positive feedback loop of chronic, inflammatory destruction of the tooth's supporting tissues. In this review, we present the latest information on the molecular architecture of the T9SS and provide mechanistic insight into its role in secretion and attachment of cargo proteins to produce a virulence coat on cells and OMVs. The recent molecular structures of the T9SS motor comprising PorL and PorM as well as the secretion pore Sov, together with advances in the overall interactome, have provided insight into the possible mechanisms of secretion. We propose the presence of PorL/M motors arranged in a circle at the inner membrane with bent periplasmic rotors interacting with the PorN protein. At the outer membrane, we envisage a slide carousel model where the PorN protein is driven around a circular track composed of PorK. Cargo proteins are transported by PorN to PorW and the Sov translocon just as slides are rotated to the projection window. Secreted proteins are proposed to then be shuttled along highways consisting of the PorV shuttle protein to an array of attachment complexes distributed around the cell. The cell surface attachment of cargo is a hallmark of the T9SS, and in *Porphyromonas gingivalis* and *Tannerella forsythia*, this attachment is achieved via covalent bonding to a linking sugar synthesized by the Wbp/Vim pathway. The cell-surface attached cargo are enriched on OMVs, which are then released from the cell.

**Keywords:** periodontal disease(s)/periodontitis, bacterial virulence, host pathogen interactions, ultrastructure, microbiology, outer membrane vesicles

## Severe Periodontitis: A Type IX Secretion System–Driven Dysbiosis?

Periodontitis is a prevalent, chronic inflammatory disease associated with a dysbiotic subgingival plaque that results in the destruction of the tooth's supporting tissues. The global prevalence of severe periodontitis has been estimated at 11.2%, and the disease is ranked the sixth most prevalent disease worldwide (Tonetti et al. 2017). The economic burden of periodontitis in the United States and Europe has been estimated as US\$342 billion (Botelho et al. 2021). Over the past 15 y, evidence has accumulated that periodontitis is linked with a range of systemic diseases such as diabetes, cardiovascular diseases, certain cancers, and dementia, suggesting that periodontal health is vital for good general health (Hajishengallis and Chavakis 2021).

The identification of bacterial species that characterize a subgingival plaque dysbiotic signature started with the seminal cross-sectional study by Socransky et al. (1998). This study was the first to show a close association of a specific bacterial consortium with severe periodontitis (Socransky et al. 1998). The consortium comprising *Porphyromonas gingivalis*, *Treponema denticola*, and *Tannerella forsythia* was referred to as the red complex as these species were found together in

deep periodontal pockets, and they were the only bacteria of the 40 bacterial taxa studied that closely associated with disease.

The technology for identification of bacterial species in dental plaque has progressed significantly since these earlier studies such that now, using next-generation sequencing (NGS) techniques, over 200 different taxa can be identified in the microbial community of a plaque sample. There are now many cross-sectional plaque microbiome studies published comparing periodontal health with disease using NGS. These microbiome studies have identified bacterial species that seem preferentially associated with health or disease, and largely

<sup>1</sup>Oral Health CRC, Melbourne Dental School, Bio21 Institute, The University of Melbourne, Victoria, Australia

<sup>2</sup>Laboratoire d'Ingénierie des Systèmes Macromoléculaires (LISM), Institut de Microbiologie, Bioénergies et Biotechnologie (IM2B), Aix-Marseille Université, Centre National de la Recherche Scientifique (CNRS), UMR7255, Marseille Cedex, France

### Corresponding Author:

E.C. Reynolds, Oral Health CRC, Melbourne Dental School, Bio21 Institute, The University of Melbourne, 720 Swanston Street, Victoria, 3010, Australia.

Email: e.reynolds@unimelb.edu.au

they have confirmed the close association of the red complex bacteria in deep periodontal pockets from patients with severe periodontitis in whom these 3 species, *P. gingivalis*, *T. denticola*, and *T. forsythia*, can be found in abundance within a complex microbial community (Kirst et al. 2015; Shi et al. 2020; Lenartova et al. 2021).

A limitation with cross-sectional analyses of subgingival plaque samples is the dynamic nature of periodontitis, in which sites may be inactive at any single sampling time; hence, prospective clinical studies are required to better link the microbial composition with disease progression. One prospective study by Byrne et al. (2009) was designed to determine the level of certain bacterial species in subgingival plaque of patients with moderate to severe periodontitis at 3 monthly intervals during a maintenance program (Byrne et al. 2009). The levels of these species at sites that progressed by losing 2 mm or greater clinical attachment could then be compared with their levels at sites that remained stable. This study confirmed the finding that the red complex bacteria were strongly associated with disease severity but importantly extended the finding by showing that the emergence of these pathogens, particularly *P. gingivalis*, preceded attachment loss, implying a direct link with disease progression. In fact, the study showed that the level of *P. gingivalis* was an excellent biomarker for disease progression at severe periodontitis sites.

These pathogenic species associated with severe periodontitis display mutualistic symbioses in metabolism, growth, and biofilm formation, as well as synergistic virulence in animal models of infection (Tan et al. 2014). In fact, animal model studies have shown that *P. gingivalis* can drive dysbiosis and that the proteases called gingipains are the major virulence factors of the bacterium. These studies have resulted in *P. gingivalis* being referred to as a keystone pathogen in periodontitis (Hajishengallis et al. 2012). Further evidence of the importance of these bacterial species in severe disease is their temporospatial relationship in the periodontal pocket. Studies investigating the architecture and temporospatial distribution of pathogens in subgingival plaque have demonstrated that species from the genera *Porphyromonas*, *Tannerella*, *Prevotella*, and *Treponema* (e.g., *P. gingivalis*, *T. forsythia*, *Prevotella intermedia*, and *T. denticola*) are found at the base of deep pockets in patients with severe periodontitis and therefore are referred to as site specialists (Kigure et al. 1995; Mark Welch et al. 2019). Metagenomic analyses of these bacteria demonstrate an expanded functionality or overrepresentation of genes encoding proteases, adhesins, iron acquisition systems, and secretion systems. In fact, it has been suggested that even though the microbiomes of severe periodontitis sites may be taxonomically heterogeneous, they are functionally congruent through the expression and secretion of functionally similar virulence factors (Shi et al. 2020; Altabtaei et al. 2021). Interestingly a common characteristic of *P. gingivalis*, *T. forsythia*, and *P. intermedia* is the newly identified Type IX Secretion System (T9SS), which these species use to load their cell surface with an array of virulence factors, including proteases, adhesins, hemolysins, and internalins (Veith et al. 2017).

These virulence factors are actively released on outer membrane vesicles (OMVs), which can then penetrate the pocket epithelium to dysregulate the host defenses (O'Brien-Simpson et al. 2009). The best example of this process is the secretion of the major virulence factors of *P. gingivalis*, the gingipains, by the T9SS.

## The T9SS Loads the Outer Membrane with Virulence Factors for a Mobilized Vesicle Army

The T9SS is a nanomachine that secretes cargo proteins from the periplasm to the cell surface of Gram-negative bacteria. The T9SS is not ubiquitous and is restricted to species belonging to the *Bacteroidetes–Chlorobi–Fibrobacteres* superphylum. All T9SS cargo proteins are translocated across the inner membrane (IM) by the Sec translocon due to their N-terminal signal sequence and are then recruited by the T9SS for secretion across the outer membrane (OM) by their structurally conserved C-terminal domain (CTD) sequence (Lasica et al. 2017; Veith et al. 2017). The cargo proteins are then attached to the cell surface via covalent linkage to A-lipopolysaccharide (A-LPS) to form a virulence coat, surrounding both cells and released OMVs. The genes required for these processes fall into 2 broad groups (Table). The first group of genes codes for components of the T9SS machinery, including IM proteins (PorL and PorM), OM associated proteins (PorE, PorF, PorG, PorK, PorN, PorP, PorQ, PorT, PorU, PorV, PorW, PorZ, and Sov) (Sato et al. 2010; Naito et al. 2019), and components involved in signal transduction and gene regulation (PorA, PorX, PorY, and SigP) (Yukitake et al. 2020). Besides PorA, all of these proteins have orthologs in *T. forsythia* and *P. intermedia* (Table). Deletion of these genes prevents the secretion, maturation, and attachment of cargo to the cell surface, resulting in nonpigmented colonies of *P. gingivalis* on a blood agar plate (Sato et al. 2010).

The second group includes genes involved in the biosynthesis of A-LPS. The polysaccharide portion of A-LPS is proposed to consist of an anionic phosphorylated branched mannan (Paramonov et al. 2015), but accumulating evidence suggests that A-LPS includes a more conventional polysaccharide requiring 4 glycosyltransferases specific for A-LPS (WbaP, GtfC, VimF, and GtfF) and 2 further glycosyltransferases (GtfE and GtfB) that are also required for the synthesis of O-polysaccharide in “O-LPS” (Shoji et al. 2018). The novel A-LPS linking sugar that is bonded to the cargo proteins was recently identified to be a 2-N-seryl-3-N-acetylglucuronamide in *P. gingivalis* and a 2-N-glycyl-3-N-acetylmannuronic acid in *T. forsythia* that is synthesized by the novel Wbp/Vim pathway comprising WbpA, UgdA, WbpB, WbpE (also known as PorR), WbpD, WbpS, VimE, and VimA (Veith et al. 2020). Deletion of A-LPS biosynthetic genes results in loss of surface attachment, with the cargo released into the growth medium (Gorasia et al. 2015) and nonpigmented colonies on blood agar (Shoji et al. 2018). *P. intermedia* does not have orthologs for several enzymes in the Wbp/Vim pathway (Table), suggesting

**Table.** T9SS-Related Genes That Are Essential for Growth or Fitness Identified by Transposon Sequencing.

Gene Name	33277 Locus Tag	W83 Locus Tag	Ortholog in <i>Pi</i> or <i>Tf</i>	Protein Description	Inherently Essential for Growth <sup>a</sup>	Essential for Fitness <sup>b</sup>
<b>T9SS components</b>						
<i>plug</i>	PGN_0144	PG2092	<i>Pi, Tf</i>	Plugs periplasmic opening of Sov	—	—
<i>porA</i> <sup>c,d</sup>	PGN_0123	PG2172	—, —	Proposed T9SS regulatory signal receptor	—	—
<i>porE</i>	PGN_1296	PG1058	<i>Pi, Tf</i>	PorP-associated lipoprotein; peptidoglycan binding domain	+	—
<i>porF</i>	PGN_1437	PG0534	<i>Pi, Tf</i>	Predicted TonB-dependent receptor	+	—
<i>porG</i>	PGN_0297	PG0189	<i>Pi, Tf</i>	Predicted 8-stranded OM $\beta$ -barrel associated with PorK/N	+	—
<i>porK</i>	PGN_1676	PG0288	<i>Pi, Tf</i>	OM lipoprotein, forms large periplasmic rings with PorN	—	—
<i>porL</i>	PGN_1675	PG0289	<i>Pi, Tf</i>	Motor stator	+	—
<i>porM</i>	PGN_1674	PG0290	<i>Pi, Tf</i>	Motor rotor and shaft	+	—
<i>porN</i>	PGN_1673	PG0291	<i>Pi, Tf</i>	Forms large periplasmic rings in association with PorK	+	—
<i>porP</i>	PGN_1677	PG0287	<i>Pi, Tf</i>	Predicted 14-stranded OM $\beta$ -barrel, binds to PorE	+	—
<i>porQ</i>	PGN_0645	PG0602	<i>Pi, Tf</i>	Attachment complex, 14-stranded OM $\beta$ -barrel, binds to PorZ	+	—
<i>porT</i>	PGN_0778	PG0751	<i>Pi, Tf</i>	Predicted 8-stranded OM $\beta$ -barrel protein	—	—
<i>porU</i> <sup>c</sup>	PGN_0022	PG0026	<i>Pi, Tf</i>	Attachment complex, T9SS sortase, binds to PorV	+	—
<i>porV</i>	PGN_0023	PG0027	<i>Pi, Tf</i>	T9SS shuttle protein and attachment complex member, 14-stranded OM $\beta$ -barrel, binds to PorU, Sov, PorA, and other cargo	+	—
<i>porW</i>	PGN_1877	PG1947	<i>Pi, Tf</i>	OM lipoprotein, forms bridge between PorN and Sov	—	—
<i>porX</i>	PGN_1019	PG0928	<i>Pi, Tf</i>	Two-component response regulator, activates SigP	+	—
<i>porY</i>	PGN_2001	PG0052	<i>Pi, Tf</i>	Two-component histidine kinase, activates PorX	+	—
<i>porZ</i> <sup>c,d</sup>	PGN_0509	PG1604	<i>Pi, Tf</i>	Attachment complex, binds to PorQ and A-LPS	—	—
<i>sigP</i>	PGN_0274	PG0162	<i>Pi, Tf</i>	Extracytoplasmic function sigma factor, $\sigma^P$	—	—
<i>sov</i>	PGN_0832	PG0809	<i>Pi, Tf</i>	T9SS translocon, gated by its binding to PorV or Plug	+	—
<b>A-LPS biosynthesis</b>						
<i>ugdA</i>	PGN_0613	PG1277	<i>Pi, Tf</i>	UDP-D-GlcNAc 6-dehydrogenase	+	E, M
<i>wbpA</i>	PGN_1243	PG1143	<i>Pi, Tf</i>	UDP-D-GlcNAc 6-dehydrogenase	+	E, M
<i>wbpB</i>	PGN_0168	PG2119	—, <i>Tf</i>	C3-dehydrogenase	—	E, M, C
<i>wbpD</i>	PGN_0002	PG0002	—, <i>Tf</i>	Acetyltransferase	—	E, M, C
<i>wbpE</i>	PGN_1236	PG1138	<i>Pi, Tf</i>	Aminotransferase	—	—
<i>wbpS</i>	PGN_1234	PG1136	—, —	Amidotransferase	+	—
<i>imE</i>	PGN_1055	PG0883	—, <i>Tf</i>	Deacetylase	—	—
<i>vimA</i>	PGN_1056	PG0882	—, <i>Tf</i>	N-seryltransferase	—	—
<i>wbaP</i>	PGN_1896	PG1964	<i>Pi, Tf</i>	Phosphoglycosyltransferase, putative transfer of first sugar of A-LPS repeating unit	+	—
<i>gtfC</i>	PGN_0242	PG0129	<i>Pi, Tf</i>	Putative rhamnosyltransferase	+	E, M
<i>gtfF</i>	PGN_1668	PG0294	<i>Pi, —</i>	Glycosyltransferase family 2	+	—
<i>vimF</i>	PGN_1054	PG0884	—, <i>Tf</i>	Glycosyltransferase family 2, putative transfer of linking sugar	+	—
<b>T9SS cargo</b>						
<i>tapA</i>	PGN_0152	PG2102		TprA-associated protein, mutant is less virulent in murine lesion model	—	E, M
<i>mfa5</i>	PGN_0291	PG0182		Tip fimbriin of Mfal fimbriae, mutation reduces Mfal fimbriae abundance	—	E, C
<i>cpg70</i>	PGN_0335	PG0232		Metalloprotease, processes gingipains, mutant less virulent in murine lesion model	—	E, C
<i>prtT</i>	PGN_0561	PG1548		Thiol protease related to periodontain	—	E, M, C
	PGN_0654	PG0611		Function unknown	—	E, M
	PGN_0657	PG0614		Function unknown	—	—
<i>hbp35</i>	PGN_0659	PG0616		Hemin binding protein with multiple virulence properties	—	—
	PGN_0693	PG0654		Function unknown	+	—
	PGN_0795	PG0769		Function unknown	—	E, M, C
	PGN_0852	PG1374		Leucine-rich repeat protein	—	E, M, C
<i>ppaD</i>	PGN_0898	PG1424		Peptidylarginine deiminase, role in rheumatoid arthritis	+	E, M, C
<i>prtT</i>	PGN_0900	PG1427		Periodontain, thiol protease and hemagglutinin, rapidly inactivates $\alpha_1$ -proteinase inhibitor of neutrophil elastase	—	E, M, C
	PGN_1115	PG1326		Hemagglutinin	—	—
	PGN_1321	PG1030		Function unknown	+	E, M, C
<i>pepK</i>	PGN_1416	PG0553		Lys-specific serine endopeptidase	—	E, M, C
<i>rgbB</i>	PGN_1466	PG0506		Arg-specific gingipain (cysteine proteinase), multiple virulence properties, less virulent in multiple animal models of disease	—	E, M, C

(continued)

Table. (continued)

Gene Name	33277 Locus Tag	W83 Locus Tag	Ortholog in <i>Pi</i> or <i>Tf</i>	Protein Description	Inherently Essential for Growth <sup>a</sup>	Essential for Fitness <sup>b</sup>
<i>inJ</i>	PGN_1476	PG0495		Function unknown	+	E, M
	PGN_1556	PG0411		Hemagglutinin	—	E, M
	PGN_1611	PG0350		Internalin, leucine-rich repeat protein, role in homotypic and heterotypic biofilm formation and epithelial cell invasion	—	E, M
<i>kgp</i>	PGN_1728	PG1844		Lys-specific gingipain (cysteine proteinase), multiple virulence properties, less virulent in multiple animal models of disease	—	—
<i>hagA</i>	PGN_1733	PG1837		Hemagglutinin	—	E, M
	PGN_1767	PG1798		Function unknown	—	—
<i>rgpA</i>	PGN_1770	PG1795		Function unknown	+	E, M
	PGN_1970	PG2024		Arg-specific gingipain (cysteine proteinase), multiple virulence properties, less virulent in multiple animal models of disease	—	E, M
	PGN_2065	PG2198		Function unknown	—	E, M
	PGN_2080	PG2216		Function unknown	+	E, M

A-LPS, A-lipopolysaccharide; GlcNAc, N-acetyl-D-glucosamine; OM, outer membrane; T9SS, Type IX Secretion System; +, essential; —, not essential.

<sup>a</sup>Found to be inherently essential in at least 1 of 3 transposon sequencing studies (Klein et al. 2012; Hutcherson et al. 2016; Miller et al. 2017).

<sup>b</sup>Found to be conditionally essential and required under defined conditions: epithelial colonization (E), murine abscess formation (M), and cigarette smoke extract exposure (C) (Miller et al. 2017; Hutcherson et al. 2020).

<sup>c</sup>Codes for a protein that is both a T9SS component and a cargo protein.

<sup>d</sup>No sequence detected in transposon sequencing output pool of 1 to 2 conditions tested for fitness.

it may use a different type of linking sugar to attach its cargo to the cell surface.

Since T9SS cargo proteins are greatly enriched in *P. gingivalis* OMVs and comprise approximately 60% of the protein content (Veith et al. 2014, 2018), OMVs can be considered an extension of the T9SS, delivering cargo into the periodontal tissues. OMVs play important roles in adaptation to stress, biofilm formation, host immunomodulation, and adherence to host cells and dysbiosis (Veith et al. 2018; Cecil et al. 2019; Zhang et al. 2020). There are many mechanisms by which OMVs are generated involving peptidoglycan biosynthesis, envelope stress response, nutrient response such as to iron limitation, regulation of OM proteins binding to peptidoglycan, and regulation of the VacJ/Yrb phospholipid (PL) import system (Schwechheimer and Kuehn 2015; Roier et al. 2016; Zhang et al. 2020).

*P. gingivalis* uses its T9SS to secrete and anchor many characterized virulence proteins to the surface of the cell, as recently reviewed (Lasica et al. 2017; Veith et al. 2017). Some of these virulence proteins are discussed below and include the abundant cysteine proteases known as gingipains (Kgp, RgpA, RgpB), which are the bacterium's major virulence factors that degrade host proteins and extract peptides for growth. The gingipains also play a major role in disease pathogenesis through dysregulation of host defense and inflammatory responses (Guo et al. 2010). Other proteases are PepK, CPG70, PrtT, and periodontain. Peptidylarginine deiminase (PPAD) is linked to rheumatoid arthritis (Gully et al. 2014). PG0350 and PG1374 are leucine-rich repeat containing proteins with homology to internalin J from *Listeria monocytogenes* and may facilitate invasion of host cells and affect mono- and heterotypic species biofilm formation. Mfa5 is 1 of 3 ancillary tip proteins

essential for assembly of the tip fimbriins of MfaI fimbriae. The T9SS and Mfa5 in particular have been shown to be essential for the recently discovered “surface translocation” of *P. gingivalis* (Moradali et al. 2019).

*P. gingivalis* is auxotrophic for heme, and the acquisition of iron plays an essential role in its growth and virulence (Smalley and Olczak 2017). The availability of iron in the host is extremely low due to strong sequestration by host hemin binding proteins such as the hemoglobin-haptoglobin complex, hemopexin, and albumin; therefore, *P. gingivalis* has evolved very efficient systems for the extraction, capture, and transportation of heme (Rangarajan et al. 2017; Smalley and Olczak 2017). An additional role of the gingipains is the extraction of heme from host proteins, converting it to the black pigmented heme dimer,  $\mu$ -oxo bisheme, and efficiently storing it on the cell surface bound to A-LPS. *P. gingivalis* has a 10-fold greater specific hemin binding affinity and greater heme storage capacity than the accessory pathogen *P. intermedia* (Tompkins et al. 1997; Socransky et al. 1998).

Recently, we have shown that A-LPS can be exchanged between different *P. gingivalis* cells through close contact or through fusion with OMVs with the potential for transfer of the bound  $\mu$ -oxo bisheme (Glew et al. 2021). This has important consequences in terms of altering the oral microbiota and may help explain why *P. gingivalis* has such a key role in pathogenesis (Hajishengallis et al. 2012). The T9SS, by loading OMVs with  $\mu$ -oxo bisheme, may enable *P. gingivalis* to affect the availability of iron for other periodontitis-related bacterial species that require hemin for growth. Thus, LPS-hemin exchange with *P. gingivalis*, particularly with its OMVs, may contribute to polymicrobial synergy in the development of a dysbiotic community.



Transposon sequencing (TnSeq) technology has enabled the genome-wide determination of *P. gingivalis* essential genes for growth and fitness. These strategies have compared the populations of saturated transposon mutagenized genes before and after planktonic growth in rich medium (Klein et al. 2012; Hutcherson et al. 2016), after colonization of oral epithelial cells (TIGK), after infection in a murine abscess model (Miller et al. 2017), or after exposure to cigarette smoke extract (Hutcherson et al. 2020). Essential genes for growth are “inherently essential” and cannot be considered for assessment for fitness in defined environments that are “conditionally essential.” The Table summarizes the *P. gingivalis* TnSeq data for T9SS-related genes that are inherently essential or required for fitness under 3 conditions. Sixty-five percent of the T9SS components and 58% of the genes specific for the biosynthesis of A-LPS were found to be essential for growth. In contrast, only 23% of T9SS cargo genes were inherently essential, but 77% were required for fitness under 1 to 3 conditions (Table). These TnSeq analyses show an important difference between T9SS component and cargo protein genes. Most T9SS components are essential for growth, but the majority of the T9SS cargo proteins are important for fitness, which exemplifies the importance of the T9SS-related genes for *P. gingivalis* survival and fitness. It also reinforces our understanding of the T9SS cargo proteins as important virulence factors.

## The T9SS Nanomachine: Molecular Architecture and Function

A fully assembled T9SS has not been isolated yet, suggesting it is a dynamic system. Nevertheless, full or partial structures and functions of many components have been elucidated. Structures of major subcomplexes, including the motor complex and the translocon, have been solved using cryo-electron microscopy (cryo-EM), and protein interactome studies are helping to form a cohesive functional picture of the T9SS as a whole as detailed below.

### The T9SS Translocon

The identity of the components that form the OM translocon was unknown until recently. Sov/SprA, a 267-kDa protein, was hypothesized to form the secretion channel in the OM based on its large size and its retention in a minimal T9SS found in some members of the *Bacteroidetes* phylum (Lauber et al. 2018). Accordingly, these authors tagged and isolated SprA-containing complexes from *Flavobacterium johnsoniae* and solved their structures by cryo-EM. Two complexes were solved, one with SprA bound to the PorV OM  $\beta$ -barrel protein and the other with SprA bound to the Plug protein (Lauber et al. 2018). SprA forms an extremely large, 36-stranded transmembrane  $\beta$ -barrel with an external cap, a lateral opening above the membrane, and an internal solvent-filled pore of approximately 70 Å, large enough to allow the secretion of folded cargo proteins. This is the largest single polypeptide

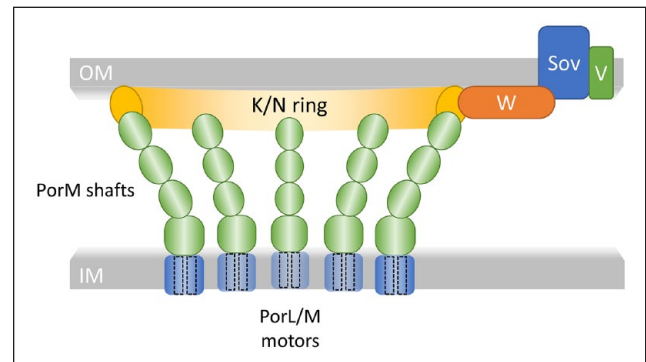


**Figure 1.** Multiple PorL/M motors form a funnel-shaped cage in the periplasm. Cross section of the trans-envelope complex showing half of a PorK/N ring in the outer membrane (OM) and a small number of PorL/M motors in the inner membrane (IM). The pentameric PorL stator is shown in blue and encloses the 2 transmembrane helices of the PorM dimer (1 from each monomer). The PorM shaft is composed of 4 periplasmic domains shown in green. Considering the abundance of PorKLMN proteins relative to each other in whole cells, the number of PorM molecules should be similar to the number of PorK and PorN molecules, which is estimated to be 32 to 36 per ring based on cryo-EM images (Gorasia et al. 2016). Since there are only 2 PorM molecules per motor complex, we predict that many motors (possibly 16–18 of them) form a ring in the IM with their bent shafts forming a dynamic funnel-shaped cage in the periplasm. One PorW subunit forms a bridge to the single translocon (Sov), which is shown bound to the PorV shuttle protein (Gorasia, Chreifi, et al. 2020).

transmembrane  $\beta$ -barrel identified to date. When bound to PorV, the lateral opening of SprA faces the extracellular loops of PorV, while in the Plug–SprA complex, the lateral opening is free, but the periplasmic entrance is blocked by the Plug protein. The authors proposed a model for the T9SS translocon mechanism whereby the 2 ends of the channel are alternately gated. In this model, the SprA–PorV complex represents the “open state” and allows uptake of the T9SS substrates from the periplasm while the SprA–Plug complex represents the state after the T9SS substrates have been released, leading to unidirectional transport of substrates through the translocon.

### The Shuttle Protein

The most abundant T9SS component is PorV, also called LptO, a 14-stranded OM  $\beta$ -barrel protein related to the family of FadL transporters (Chen et al. 2011; Gorasia, Glew, et al. 2020). As mentioned above, PorV associates with the T9SS translocon, and additionally, PorV binds to T9SS substrates harboring a CTD signal (Glew et al. 2017). Given that the only known similarity among the T9SS cargo is the presence of the CTD signal, it was suggested that PorV binds to the CTD signal, enabling it to collect substrates from the translocon and shuttle them to the attachment complexes (discussed below) (Glew et al. 2017). This theory was elegantly supported by the work of Lauber et al. (2018), in which a long extracellular loop of PorV was found to penetrate inside the lumen of the SprA pore, suggesting PorV collects the T9SS substrates directly from the translocon. However, it is unclear whether

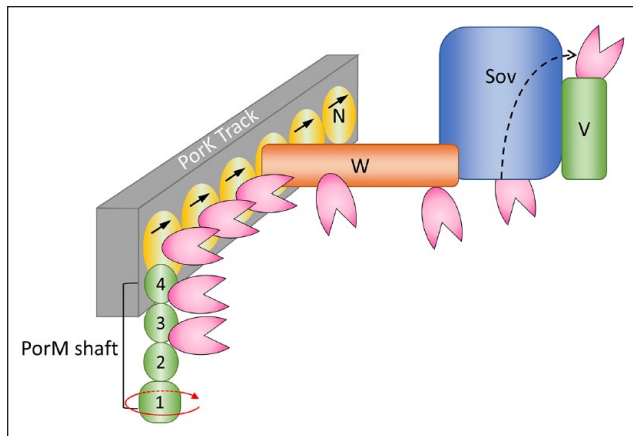


**Figure 2.** Proposed cargo delivery from PorM to PorV. The spatial organization of the Type IX Secretion System (Gorasia, Chreifi, et al. 2020, unpublished) together with data showing that the C-terminal domain signals of cargo proteins interact with PorM, PorN and PorW (Vincent et al. 2018, unpublished) suggest a pathway for the delivery of cargo to the secretion pore. The cargo (pink) are recruited by the rotating shafts of PorM (green) and passed to PorN (yellow). PorN is proposed to physically move along the PorK track (gray), transporting the cargo with it. At one point along the circular track, the cargo is passed to PorW (orange) and then to the Sov translocon (blue). The cargo is secreted through Sov and delivered to the PorV shuttle protein (green). Note that the track is shown as a straight block since it has not yet been determined whether Sov and PorV are on the inside or outside of the ring.

substrate-bound PorV moves through the OM to reach an attachment complex or whether the T9SS substrate gets passed along a chain of PorV molecules on the cell surface.

### The Attachment Complex

Most of the T9SS cargo proteins in *P. gingivalis* are attached to the cell surface. It is known that T9SS substrates are modified with A-LPS, explaining cell attachment, but the exact mechanism of how this occurred was unclear until recently. The 440-kDa attachment complex, comprising the PorU and PorZ surface proteins and the PorV and PorQ OM  $\beta$ -barrels, was identified using blue native gel electrophoresis (Glew et al. 2017). Both PorU and PorZ possess a CTD signal and use the T9SS to reach the cell surface. However, rather than being processed and conjugated to A-LPS (Glew et al. 2012; Lasica et al. 2016), PorU and PorZ are anchored to the OM through their binding to PorV and PorQ, respectively (Glew et al. 2017). The crystal structure of PorZ showed that it consists of 2  $\beta$ -propeller domains in addition to its CTD (Lasica et al. 2016). The proposed function of PorZ was to bind carbohydrate/A-LPS (Lasica et al. 2016; Glew et al. 2017), which was confirmed by detecting the specific binding of recombinant PorZ to A-LPS (Madej et al. 2021). Furthermore, PorZ interacts with PorU in an A-LPS-dependent manner, supporting a role for PorZ in presenting the A-LPS substrate to PorU (Madej et al. 2021). The catalytic component of the attachment system, PorU, uses a sortase-like mechanism to cleave the CTD signal at the cell surface and covalently attach the A-LPS linking sugar (see above) to the new C-terminus of the cargo proteins via a peptide bond (Glew et al. 2012; Gorasia

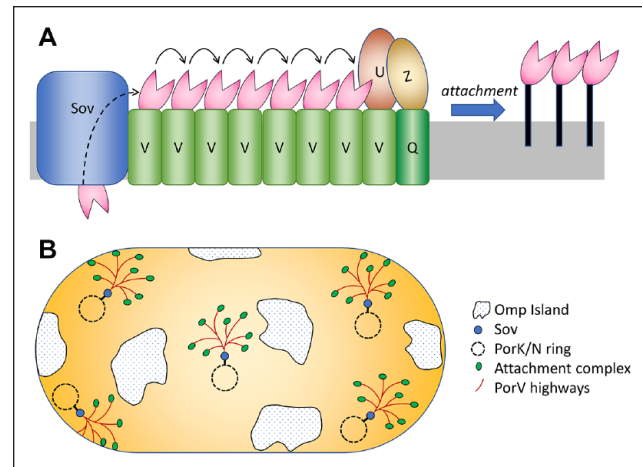


**Figure 3.** Proposed mechanism and pathway of cargo delivery to the attachment complexes. The delivery of cargo from the translocon (Sov) to the attachment complex composed of PorU, PorV, PorZ, and PorQ is an outstanding question of considerable interest. This figure is a speculative model that assumes that this process occurs outside of the PorK/N rings. **(A)** Once secreted and bound to PorV, the cargo (pink) are proposed to be passed along a series of PorV molecules until they reach an attachment complex, where they are processed to become permanently attached to the outer membrane (OM) via conjugation to A-lipopolysaccharide (A-LPS). The PorV chain may be continuous (as depicted) or may have gaps requiring short diffusion distances to be covered. In this latter case, the PorV–PorV interactions may be dynamic. **(B)** In the context of a whole cell, we envisage a tree-like arrangement of PorV highways that connect a small number of translocation systems to a much larger number of attachment complexes at a ratio of approximately 1:8 (Glew et al. 2017). The major OM proteins of Gram-negative bacteria are known to be organized into “Omp islands,” which are areas of extremely low diffusion (Chavent et al. 2018). The Type IX Secretion System shuttle system would be located outside of these areas, where there is higher diffusion and where the OM has more freedom to bulge out and form outer membrane vesicles.

et al. 2015; Veith et al. 2020). This results in permanent anchorage of the T9SS substrates to the cell surface.

### The Proposed T9SS Powertrain

PorK, PorL, PorM, and PorN together form a trans-envelope complex (Sato et al. 2010; Vincent et al. 2017), which appears to be anchored to the peptidoglycan layer via the PorP–PorE complex (Gorasia, Chreifi, et al. 2020; Gorasia, Veith, and Reynolds 2020). The PorP component was shown to interact with the trans-envelope complex (Vincent et al. 2017), while PorE was shown to associate with the peptidoglycan (Trinh et al. 2020). Cryo-EM analysis of a purified complex containing PorK, PorN, and PorG showed that these 3 proteins form large 50-nm ring-like structures (Gorasia et al. 2016). Biochemical evidence suggested that the PorK/N ring was localized in the periplasm and tethered to the OM, a location supported by recent in situ images from cryo-EM (Gorasia, Chreifi, et al. 2020). Although the PorK/N ring and PorL/M motor are purified as separate complexes, PorM is known to interact with the ring proteins (Vincent et al. 2017).

The structure of the molecular motor that drives secretion and gliding motility was solved by cryo-EM and found to be

composed of a PorL pentamer associated with a PorM dimer. In total, 10  $\alpha$ -helices from PorL form the “stator,” which is membrane embedded and surrounds the 2 transmembrane helices of the PorM “rotor” and causes them to rotate by using energy from the proton motive force (Hennell James et al. 2021). The periplasmic domains of PorM form a bent shaft that traverses the periplasm and at the tip is calculated to rotate around a circle of 18 nm, where it may drive processes at the OM through its contact with the PorK/N rings (Sato et al. 2020; Hennell James et al. 2021). The *porKLMN* transcription unit is well conserved among bacteria, which use the T9SS supporting the proposed flow of energy from the motor complex to the PorK/N ring.

While the motor has 5 subunits of PorL and 2 subunits of PorM, the PorK/N ring has 32 to 36 subunits of each component (Gorasia et al. 2016). Given the relative whole cell abundance of these proteins is approximately 1 PorK to 3 PorL to 1 PorM to 1 PorN (Glew et al. 2017; Gorasia, Glew, et al. 2020), there is likely to be a ring of motors directly underneath the PorK/N ring to form a symmetrical funnel-shaped cage in the periplasm (Fig. 1).

Until recently, the Sov translocon had no known connection to the PorKLMN system, such that the pathway of energy provision for secretion was unclear. Recently, we provided evidence that PorW connects these 2 disparate complexes in *P. gingivalis* and have now confirmed direct interactions between PorW and PorN and also between PorW and Sov (Gorasia, Chreifi, et al. 2020; Gorasia, Lunar Silva, et al. unpublished). For the first time, these interactions map out a potential pathway for energy transduction to the Sov translocon. In addition, this same interactome maps out a pathway for the delivery of cargo to the translocon since the CTD signal of multiple cargo proteins have been shown to interact with PorM, PorN, and PorW (Vincent et al. 2018; Lunar Silva et al. unpublished).

The emerging design suggests that cargo proteins are recruited by the rotating the PorM shaft and transferred to PorN. PorN may in turn be physically moved around the fixed circular track composed of PorK and deliver the cargo to PorW, like slides are delivered to the projection window in a slide carousel. PorW would then transfer the cargo to the secretion pore Sov (Fig. 2). This design enables cargo to be recruited from a large catchment volume and be delivered to the secretion pore in potentially high concentrations. This concentration effect alone may be the “energy transduction” that drives secretion, or else PorN may also transfer mechanical energy through its interaction with PorW. This scheme may also accommodate gliding motility, which has been shown to use a helical track along which motility adhesins flow (Nakane et al. 2013). To convert the circular track into a helical one, it may be sufficient

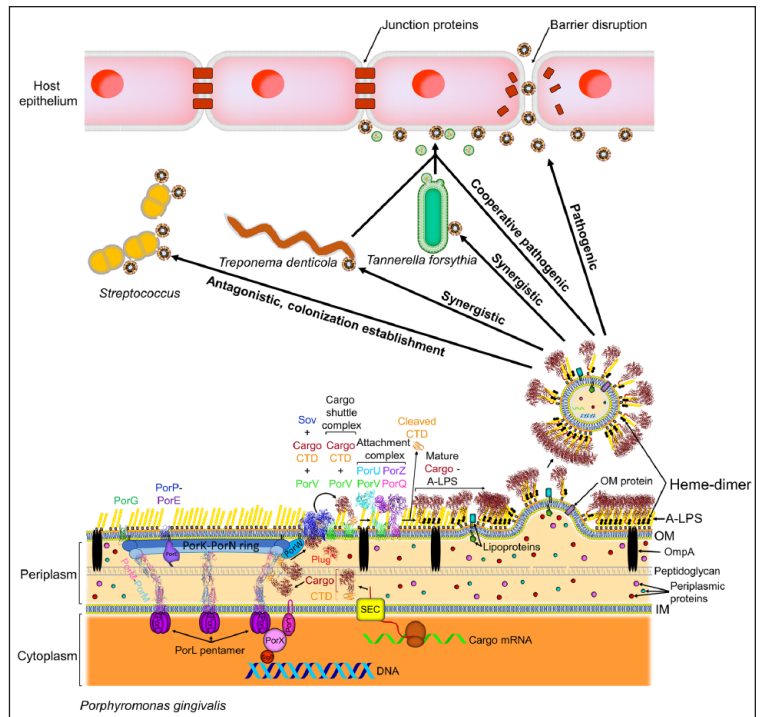


**Figure 4.** A working model of pathogenic mechanisms mediated by outer membrane vesicles (OMVs) loaded with virulence factors secreted by the Type IX Secretion System (T9SS). *Porphyromonas gingivalis* secretes and attaches cargo proteins to A-lipopolysaccharide (A-LPS) to form a virulent coat on the surface of the cell using the T9SS. The 2-component system, PorY and PorX, activate the SigP sigma factor to control the expression of many T9SS-related genes. The cargo proteins are first secreted through the Sec translocon via their N-terminal leader sequence and then are transported to Sov via C-terminal domain (CTD) binding to various PorM domains followed by binding to PorW, which anchors Sov to the PorN–PorK ring. This transport requires the proton motive force harnessed by the inner membrane (IM) helices of PorL and PorM forming the motor. Removal of the plug from Sov allows the CTD of the cargo protein to enter the exposed periplasmic Sov opening, where it binds to surface loop(s) of docked PorV at the external-side Sov opening. The CTD–cargo protein bound to PorV is released to the surface and delivered to the attachment complex, where PorU cleaves off the CTD and covalently links the new C-terminus via transpeptidation to the 2-N-seryl-3-N-acetylglucuronamide of A-LPS that is recruited by PorZ. PorU and PorZ are anchored to the outer membrane (OM) by PorQ and PorV, respectively. Due to environmental signals, such as iron limitation, these secreted cargo proteins are then packaged into OMVs, which are released into the surroundings, where they can act at a considerable distance from the source cell. *P. gingivalis* can interact antagonistically toward some bacteria, for example, through the disruption of oral streptococcal biofilms by gingipains enriched on the surface of OMVs. The  $\mu$ -oxo bisheme is extracted from the host through the action of surface gingipains on cells and OMVs and stored on the surface by binding to A-LPS. The heme-loaded OMVs can then disperse to synergistically promote the growth of other subgingival microbiota, via fusion with their OMs and exchange of heme-bound A-LPS. This alters the oral microbiota and proportion of virulence factors to cooperatively promote disease: by disrupting the epithelial barrier due to degradation of the tight junctions between host cells, increasing host cell invasion and causing dysbiosis of host systems, ultimately leading to chronic inflammation and the destruction of the tooth-supporting tissues, including bone. Structures for Plug (red, PDB ID: 6H3J) and Sov\_PorV (blue\_light green, PDB ID: 6H3I) complexes, as well as the PorM–PorL motor (hot pink + cornflower blue\_purple, PDB ID: 6ys8), were determined by cryo-electron microscopy (cryo-EM) (Lauber et al. 2018; Hennell James et al. 2021). The crystal structures for mature RgpB (PDB ID: 1CVR) and RgpB CTD (PDB ID: 5AG9) were used for the cargo proteins. PorZ (purple) and PorM dimer (hot pink + cornflower blue) were from crystal structures (PDB ID: 5ml1 [Lasica et al. 2016] and PDB ID: 7cmg [Sato et al. 2020], respectively). PorG (dark green), PorP (medium blue), PorV (light green), and PorQ (magenta)  $\beta$ -barrel structures are from Phyre2 models using amino acid sequences without N-terminal signal peptides. The PorU structure is a Phyre2 model without a signal peptide or domain A (Glew et al. 2012). Attachment and cargo shuttle complexes are depicted based on composition of complexes and subcomplexes (Glew et al. 2017).



just to add an additional component to the track. The gliding-specific GldJ lipoprotein, which shares homology with GldK/PorK, is a perfect candidate for this role and has already been suggested to form the helical track in *F. johnsoniae* (Braun and McBride 2005).

## Formation of the Virulence Coat

An intriguing and unique element of the T9SS is the attachment of numerous cargo proteins to the cell surface via A-LPS to produce a “virulence coat” around the cell. We initially thought that both the translocon and the attachment complexes would be located within the PorK/N rings, which would make the work of the PorV shuttle protein more efficient by limiting its distance of diffusion (Gorasia, Chreifi, et al. 2020). However, with the PorK/N rings implicated in energy transduction and substrate delivery, the barrier theory is no longer required to explain their function. Furthermore, it is known that PorV and other attachment complex members are highly enriched in OMVs, whereas PorK, PorN, PorW, and Sov are not (Veith et al. 2014), and therefore, for the barrier theory to be correct, OMVs would need to be formed preferentially from the OM immediately above and inside the PorK/N rings, which we have found no evidence for and seems unlikely. It is likely, then, that Sov together with PorV and the attachment system are located outside the PorK/N rings (Figs. 1 and 2). Furthermore, we have developed a mechanistic model for the cargo shuttle process, which greatly extends the cell surface area serviced by the attachment system (Fig. 3). The PorV barrels are proposed to interact laterally to form branching chains that interconnect each Sov translocon with multiple attachment complexes. The cargo proteins are passed along the PorV chains until they reach an attachment complex where they are anchored to A-LPS and released (Fig. 3). The basis for this idea is 3-fold. First, lateral interactions between OM  $\beta$ -barrels are common, for example, in porin trimers in other species (Ma et al. 2018) and in the RagAB peptide transporter of *P. gingivalis* (Madej et al. 2020), making the idea of lateral interactions between adjacent PorV molecules plausible. Second, lateral interactions involving PorV are already known to occur for the Sov–PorV complex (Lauber et al. 2018), and lateral interactions between PorV and PorQ in the attachment complexes also seem likely to help hold the complexes together. And third, passing substrates along a PorV chain obviates the need for an unlikely bidirectional highway of PorV molecules diffusing through the membrane to load and offload the cargo. Our model also considers the relative whole-cell stoichiometry recently shown to be approximately 1 PorK/N ring to 8 attachment complexes to 100 PorV molecules (Glew et al. 2017; Gorasia, Glew, et al. 2020).

## Conclusion

The dynamic nature of periodontitis can be explained by the temporospatial emergence of periodontal pathogens at the base of a periodontal pocket. These pathogens secrete virulence

factors using the T9SS and then release them into host tissue on OMVs to dysregulate the immune defense to generate a destructive, chronic, inflammatory response in a positive feedback loop to progress disease (Fig. 4). The mechanisms by which the T9SS loads virulence factors onto the surface of cells and OMVs appear to involve a novel circular conveyor belt to deliver energy and cargo proteins (virulence factors) from the motor to the secretion pore and then to the surface for attachment.

## Author Contributions

P.D. Veith, M.D. Glew, D.G. Gorasia, E. Cascales, E.C. Reynolds, contributed to conception, design, data acquisition, analysis, and interpretation, drafted and critically revised the manuscript; E. Cascales, contributed to data acquisition, analysis, and interpretation, critically revised the manuscript. All authors gave final approval and agree to be accountable for all aspects of the work.

## Declaration of Conflicting Interests

The authors declared no potential conflicts of interest with respect to the research, authorship, and/or publication of this article.

## Funding

The authors disclosed receipt of the following financial support for the research, authorship, and/or publication of this article: This work was supported by the Australian National Health and Medical Research Council grants ID 1123866 and 1193647 and the Australian Research Council grant DP200100914.

## References

- Altatbaei K, Maney P, Ganesan SM, Dabdoub SM, Nagaraja HN, Kumar PS. 2021. Anna Karenina and the subgingival microbiome associated with periodontitis. *Microbiome*. 9(1):97.
- Botelho J, Machado V, Leira Y, Proenca L, Chambrone L, Mendes JJ. 2021. Economic burden of periodontitis in the United States and Europe—an updated estimation. *J Periodontol* [epub ahead of print 30 May 2021]. doi:10.1002/JPER.21-0111
- Braun TF, McBride MJ. 2005. *Flavobacterium johnsoniae* GldJ is a lipoprotein that is required for gliding motility. *J Bacteriol*. 187(8):2628–2637.
- Byrne SJ, Dashper SG, Darby IB, Adams GG, Hoffmann B, Reynolds EC. 2009. Progression of chronic periodontitis can be predicted by the levels of *Porphyromonas gingivalis* and *Treponema denticola* in subgingival plaque. *Oral Microbiol Immunol*. 24(6):469–477.
- Cecil JD, Sirisaengtaksin N, O'Brien-Simpson NM, Krachler AM. 2019. Outer membrane vesicle–host cell interactions. *Microbiol Spectr*. 7(1):10.1128/microbiolspec.PSIB-0001-2018.
- Chavent M, Duncan AL, Rassam P, Birkholz O, Helie J, Reddy T, Beliaev D, Hambly B, Piehler J, Kleanthous C, et al. 2018. How nanoscale protein interactions determine the mesoscale dynamic organisation of bacterial outer membrane proteins. *Nat Commun*. 9(1):2846.
- Chen YY, Peng B, Yang Q, Glew MD, Veith PD, Cross KJ, Goldie KN, Chen D, O'Brien-Simpson N, Dashper SG, et al. 2011. The outer membrane protein LptO is essential for the O-deacylation of LPS and the co-ordinated secretion and attachment of A-LPS and CTD proteins in *Porphyromonas gingivalis*. *Mol Microbiol*. 79(5):1380–1401.
- Glew MD, Gorasia DG, McMillan PJ, Butler CA, Veith PD, Reynolds EC. 2021. Complementation *in trans* of *Porphyromonas gingivalis* lipopolysaccharide biosynthetic mutants demonstrates lipopolysaccharide exchange. *J Bacteriol*. 203(10):e00631-20.
- Glew MD, Veith PD, Chen D, Gorasia DG, Peng B, Reynolds EC. 2017. PorV is an outer membrane shuttle protein for the Type IX Secretion System. *Sci Rep*. 7(1):8790.



- Glew MD, Veith PD, Peng B, Chen YY, Gorasia DG, Yang Q, Slakeski N, Chen D, Moore C, Crawford S, et al. 2012. PG0026 is the C-terminal signal peptidase of a novel secretion system of *Porphyromonas gingivalis*. *J Biol Chem*. 287(29):24605–24617.
- Gorasia DG, Chreifi G, Seers CA, Butler CA, Heath JE, Glew MD, McBride MJ, Subramanian P, Kjaer A, Jensen GJ, et al. 2020. *In situ* structure and organisation of the Type IX Secretion System. *bioRxiv*. <https://www.biorxiv.org/content/10.1101/2020.05.13.094771v1>. Preprint.
- Gorasia DG, Glew MD, Veith PD, Reynolds EC. 2020. Quantitative proteomic analysis of the Type IX Secretion System mutants in *Porphyromonas gingivalis*. *Mol Oral Microbiol*. 35(2):78–84.
- Gorasia DG, Veith PD, Chen D, Seers CA, Mitchell HA, Chen YY, Glew MD, Dashper SG, Reynolds EC. 2015. *Porphyromonas gingivalis* type IX secretion substrates are cleaved and modified by a sortase-like mechanism. *PLoS Pathog*. 11(9):e1005152.
- Gorasia DG, Veith PD, Hanssen EG, Glew MD, Sato K, Yukitake H, Nakayama K, Reynolds EC. 2016. Structural insights into the PorK and PorN components of the *Porphyromonas gingivalis* Type IX Secretion System. *PLoS Pathog*. 12(8):e1005820.
- Gorasia DG, Veith PD, Reynolds EC. 2020. The Type IX Secretion System: advances in structure, function and organisation. *Microorganisms*. 8(8):1173.
- Gully N, Bright R, Marino V, Marchant C, Cantley M, Haynes D, Butler C, Dashper S, Reynolds E, Bartold M. 2014. *Porphyromonas gingivalis* peptidylarginine deiminase, a key contributor in the pathogenesis of experimental periodontal disease and experimental arthritis. *PLoS One*. 9(6):e100838.
- Guo Y, Nguyen KA, Potempa J. 2010. Dichotomy of gingipains action as virulence factors: from cleaving substrates with the precision of a surgeon's knife to a meat chopper-like brutal degradation of proteins. *Periodontol* 2000. 54(1):15–44.
- Hajishengallis G, Chavakis T. 2021. Local and systemic mechanisms linking periodontal disease and inflammatory comorbidities. *Nat Rev Immunol*. 21(7):426–440.
- Hajishengallis G, Darveau RP, Curtis MA. 2012. The keystone-pathogen hypothesis. *Nat Rev Microbiol*. 10(10):717–725.
- Hennell James R, Deme JC, Kjr A, Alcock F, Silale A, Lauber F, Johnson S, Berks BC, Lea SM. 2021. Structure and mechanism of the proton-driven motor that powers type 9 secretion and gliding motility. *Nat Microbiol*. 6(2):221–233.
- Hutcherson JA, Gogenini H, Lamont GJ, Miller DP, Nowakowska Z, Lasica AM, Liu C, Potempa J, Lamont RJ, Yoder-Himes D, et al. 2020. *Porphyromonas gingivalis* genes conferring fitness in a tobacco-rich environment. *Mol Oral Microbiol*. 35(1):10–18.
- Hutcherson JA, Gogenini H, Yoder-Himes D, Hendrickson EL, Hackett M, Whiteley M, Lamont RJ, Scott DA. 2016. Comparison of inherently essential genes of *Porphyromonas gingivalis* identified in two transposon-sequencing libraries. *Mol Oral Microbiol*. 31(4):354–364.
- Kigure T, Saito A, Seida K, Yamada S, Ishihara K, Okuda K. 1995. Distribution of *Porphyromonas gingivalis* and *Treponema denticola* in human subgingival plaque at different periodontal pocket depths examined by immunohistochemical methods. *J Periodontol Res*. 30(5):332–341.
- Kirst ME, Li EC, Alfant B, Chi YY, Walker C, Magnusson I, Wang GP. 2015. Dysbiosis and alterations in predicted functions of the subgingival microbiome in chronic periodontitis. *Appl Environ Microbiol*. 81(2):783–793.
- Klein BA, Tenorio EL, Lazinski DW, Camilli A, Duncan MJ, Hu LDT. 2012. Identification of essential genes of the periodontal pathogen *Porphyromonas gingivalis*. *BMC Genomics*. 13:578.
- Lasica AM, Goulas T, Mizgalska D, Zhou X, de Diego I, Ksiazek M, Madej M, Guo Y, Guevara T, Nowak M, et al. 2016. Structural and functional probing of PorZ, an essential bacterial surface component of the type-IX secretion system of human oral-microbiome *Porphyromonas gingivalis*. *Sci Rep*. 6:37708.
- Lasica AM, Ksiazek M, Madej M, Potempa J. 2017. The Type IX Secretion System (T9SS): highlights and recent insights into its structure and function. *Front Cell Infect Microbiol*. 7:215.
- Lauber F, Deme JC, Lea SM, Berks BC. 2018. Type 9 Secretion System structures reveal a new protein transport mechanism. *Nature*. 564(7734):77–82.
- Lenartova M, Tesinska B, Janatova T, Hrebicek O, Mysak J, Janata J, Najmanova L. 2021. The oral microbiome in periodontal health. *Front Cell Infect Microbiol*. 11:629723.
- Ma H, Khan A, Nangia S. 2018. Dynamics of *OmpF* trimer formation in the bacterial outer membrane of *Escherichia coli*. *Langmuir*. 34(19):5623–5634.
- Madej M, Nowakowska Z, Ksiazek M, Lasica AM, Mizgalska D, Nowak M, Jacula A, Bzowska M, Scavenius C, Enghild JJ, et al. 2021. PorZ, an essential component of the Type IX Secretion System of *Porphyromonas gingivalis*, delivers anionic lipopolysaccharide to the PorU sortase for transpeptidase processing of T9SS cargo proteins. *mBio*. 12(1):e02262–20.
- Madej M, White JBR, Nowakowska Z, Rawson S, Scavenius C, Enghild JJ, Bereta GP, Pothula K, Kleinekathoer U, Basle A, et al. 2020. Structural and functional insights into oligopeptide acquisition by the RagAB transporter from *Porphyromonas gingivalis*. *Nat Microbiol*. 5(8):1016–1025.
- Mark Welch JL, Dewhirst FE, Borisy GG. 2019. Biogeography of the oral microbiome: the site-specialist hypothesis. *Annu Rev Microbiol*. 73:335–358.
- Miller DP, Hutcherson JA, Wang Y, Nowakowska ZM, Potempa J, Yoder-Himes DR, Scott DA, Whiteley M, Lamont RJ. 2017. Genes contributing to *Porphyromonas gingivalis* fitness in abscess and epithelial cell colonization environments. *Front Cell Infect Microbiol*. 7:378.
- Moradali MF, Ghods S, Angelini TE, Davey ME. 2019. Amino acids as wetting agents: surface translocation by *Porphyromonas gingivalis*. *ISME J*. 13(6):1560–1574.
- Naito M, Tominaga T, Shoji M, Nakayama K. 2019. PGN\_0297 is an essential component of the Type IX Secretion System (T9SS) in *Porphyromonas gingivalis*: Tn-seq analysis for exhaustive identification of T9SS-related genes. *Microbiol Immunol*. 63(1):11–20.
- Nakane D, Sato K, Wada H, McBride MJ, Nakayama K. 2013. Helical flow of surface protein required for bacterial gliding motility. *Proc Natl Acad Sci U S A*. 110(27):11145–11150.
- O'Brien-Simpson NM, Pathirana RD, Walker GD, Reynolds EC. 2009. *Porphyromonas gingivalis* RgpA-Kgp proteinase-adhesion complexes penetrate gingival tissue and induce proinflammatory cytokines or apoptosis in a concentration-dependent manner. *Infect Immun*. 77(3):1246–1261.
- Paramonov N, Aduse-Opoku J, Hashim A, Rangarajan M, Curtis MA. 2015. Identification of the linkage between A-polysaccharide and the core in the A-lipopolysaccharide of *Porphyromonas gingivalis* W50. *J Bacteriol*. 197(10):1735–1746.
- Rangarajan M, Aduse-Opoku J, Paramonov NA, Hashim A, Curtis MA. 2017. Hemin binding by *Porphyromonas gingivalis* strains is dependent on the presence of A-LPS. *Mol Oral Microbiol*. 32(5):365–374.
- Roier S, Zingl FG, Cakar F, Durakovic S, Kohl P, Eichmann TO, Klug L, Gadermaier B, Weinzerl K, Prassl R, et al. 2016. A novel mechanism for the biogenesis of outer membrane vesicles in Gram-negative bacteria. *Nat Commun*. 7:10515.
- Sato K, Naito M, Yukitake H, Hirakawa H, Shoji M, McBride MJ, Rhodes RG, Nakayama K. 2010. A protein secretion system linked to *Bacteroidete* gliding motility and pathogenesis. *Proc Natl Acad Sci U S A*. 107(11):276–281.
- Sato K, Okada K, Nakayama K, Imada K. 2020. PorM, a core component of bacterial Type IX Secretion System, forms a dimer with a unique kinked-rod shape. *Biochem Biophys Res Commun*. 532(1):114–119.
- Schwechheimer C, Kuehn MJ. 2015. Outer-membrane vesicles from Gram-negative bacteria: biogenesis and functions. *Nat Rev Microbiol*. 13(10):605–619.
- Shi B, Lux R, Klokkevold P, Chang M, Barnard E, Haake S, Li H. 2020. The subgingival microbiome associated with periodontitis in type 2 diabetes mellitus. *ISME J*. 14(2):519–530.
- Shoji M, Sato K, Yukitake H, Kamaguchi A, Sasaki Y, Naito M, Nakayama K. 2018. Identification of genes encoding glycosyltransferases involved in lipopolysaccharide synthesis in *Porphyromonas gingivalis*. *Mol Oral Microbiol*. 33(1):68–80.
- Smalley JW, Olczak T. 2017. Heme acquisition mechanisms of *Porphyromonas gingivalis*—strategies used in a polymicrobial community in a heme-limited host environment. *Mol Oral Microbiol*. 32(1):1–23.
- Socransky SS, Haffajee AD, Cugini MA, Smith C, Kent RL Jr. 1998. Microbial complexes in subgingival plaque. *J Clin Periodontol*. 25(2):134–144.
- Tan KH, Seers CA, Dashper SG, Mitchell HL, Pyke JS, Meuric V, Slakeski N, Cleal SM, Chambers JL, McConville MJ, et al. 2014. *Porphyromonas gingivalis* and *Treponema denticola* exhibit metabolic symbioses. *PLoS Pathog*. 10(3):e1003955.
- Tompkins GR, Wood DP, Birchmeier KR. 1997. Detection and comparison of specific hemin binding by *Porphyromonas gingivalis* and *Prevotella intermedia*. *J Bacteriol*. 179(3):620–626.
- Tonetti MS, Jepsen S, Jin L, Otomo-Corgel J. 2017. Impact of the global burden of periodontal diseases on health, nutrition and wellbeing of mankind: a call for global action. *J Clin Periodontol*. 44(5):456–462.
- Trinh NTT, Tran HQ, Van Dong Q, Cambillau C, Roussel A, Leone P. 2020. Crystal structure of Type IX secretion system PorE C-terminal domain from *Porphyromonas gingivalis* in complex with a peptidoglycan fragment. *Sci Rep*. 10(1):7384.
- Veith PD, Chen YY, Gorasia DG, Chen D, Glew MD, O'Brien-Simpson NM, Cecil JD, Holden JA, Reynolds EC. 2014. *Porphyromonas gingivalis* outer

- membrane vesicles exclusively contain outer membrane and periplasmic proteins and carry a cargo enriched with virulence factors. *J Proteome Res.* 13(5):2420–2432.
- Veith PD, Glew MD, Gorasia DG, Reynolds EC. 2017. Type IX secretion: the generation of bacterial cell surface coatings involved in virulence, gliding motility and the degradation of complex biopolymers. *Mol Microbiol.* 106(1):35–53.
- Veith PD, Luong C, Tan KH, Dashper SG, Reynolds EC. 2018. Outer membrane vesicle proteome of *Porphyromonas gingivalis* is differentially modulated relative to the outer membrane in response to heme availability. *J Proteome Res.* 17(7):2377–2389.
- Veith PD, Shoji M, O'Hair RAJ, Leeming MG, Nie S, Glew MD, Reid GE, Nakayama K, Reynolds EC. 2020. Type IX Secretion System cargo proteins are glycosylated at the C terminus with a novel linking sugar of the Wbp/Vim pathway. *Mbio.* 11(5):e01497-20.
- Vincent MS, Canestrari MJ, Leone P, Stathopoulos J, Ize B, Zoued A, Cambillau C, Kellenberger C, Roussel A, Cascales E. 2017. Characterization of the *Porphyromonas gingivalis* type IX secretion trans-envelope PorKLMNP core complex. *J Biol Chem.* 292(8):3252–3261.
- Vincent MS, Chabaliere M, Cascales E. 2018. A conserved motif of *Porphyromonas* Type IX secretion effectors C-terminal secretion signal specifies interactions with the PorKLMN core complex. *bioRxiv.* <https://doi.org/10.1101/483123>. Preprint.
- Yukitake H, Shoji M, Sato K, Handa Y, Naito M, Imada K, Nakayama K. 2020. PorA, a conserved C-terminal domain-containing protein, impacts the PorXY-SigP signaling of the Type IX Secretion System. *Sci Rep.* 10(1):21109.
- Zhang Z, Liu D, Liu S, Zhang S, Pan Y. 2020. The role of *Porphyromonas gingivalis* outer membrane vesicles in periodontal disease and related systemic diseases. *Front Cell Infect Microbiol.* 10:585917.